THE ASTRONOMICAL JOURNAL, 122:908–920, 2001 August

A REEXAMINATION OF THE DISTRIBUTION OF GALACTIC FREE ELECTRONS

GILBERTO C. GÓMEZ,[1] ROBERT A. BENJAMIN, AND DONALD P. COX
Department of Physics, University of Wisconsin–Madison, 1150 University Avenue, Madison, WI 53706; gomez@wisp.physics.wisc.edu, benjamin@wisp.physics.wisc.edu, cox@wisp.physics.wisc.edu
Received 2001 April 23; accepted 2001 May 9

ABSTRACT

We present a list of 109 pulsars with independent distance information compiled from the literature. Since the compilation of Frail & Weisberg, there are 35 pulsars with new distance estimates and 25 pulsars for which the distance or distance uncertainty have been revised. We used this data to fit a smooth, axisymmetric, two-disk model of the distribution of Galactic electrons. The two exponential model components have mean local midplane densities at the solar circle of 2.03×10^{-2} and 0.71×10^{-2} cm^{-3}, and scale heights of 1.07 and 0.053 kpc. The thick component shows very little radial variation, while the second has a radial scale length of only a few kiloparsecs. We also examined a model that varies as $\mathrm{sech}^2 x$, rather than $\exp(-x)$, in both the radial and vertical directions. We prefer this model with no midplane cusp but find that the fit parameters essentially describe the same electron distribution. The distances predicted by this distribution have a similar scatter to that produced by the more complex model of Taylor & Cordes. We examine the pulsars that deviate strongly from this model. There are two regions of enhanced dispersion measure, one of which correlates well with the Sagittarius-Carina spiral arm. We find that the scatter of the observed dispersion measure from the model is not fitted well by either a normal or a lognormal distribution of lump sizes but may be caused instead by the uncertainties in the distances.

Key words: galaxies: ISM — Galaxy: structure — H II regions — ISM: general — pulsars: general

1. INTRODUCTION

One of the most important discoveries in the study of the interstellar medium is the realization that the warm ionized medium (WIM) is a major component of our Galaxy; it has a thick distribution and is not localized around ionization sources. Reynolds (1989) used the dispersion measures ($\mathrm{DM} = \int n_e\, dl$) toward pulsars with known distances to measure the scale height of the WIM in the Milky Way, showing that it is much larger than that of the bulk of the neutral hydrogen.

If the distance to a pulsar is known, this can be used with its DM to constrain models for the spatial distribution of the free electrons. The most popular model is that derived by Taylor & Cordes (1993, hereafter TC), which also used the observed scattering measures to a set of pulsars to refine the parameters of the model. Their most important contribution was the addition of nonaxisymmetric elements, i.e., spiral arms defined by the locations of H II regions (Georgelin & Georgelin 1976). Their main justification is the observed asymmetry in the DM versus Galactic longitude plots. They also incorporated the unusually high DM observed toward the Gum Nebula.

Models of this kind are used frequently to determine distances to pulsars. TC claim that their model yields distances accurate to 25%. But, since its publication, the set of pulsars with independent distance measurement has increased, some distances have been revised, and pulsars with forbidden DM (higher than the asymptotic value predicted by TC) have been observed. In addition, observations of the angular broadening of radio sources have been used to constrain the electron density in the Galactic center (Lazio et al. 1999; Lazio & Cordes 1998c, 1998d) and the scale length of the distribution in the anticenter direction (Lazio & Cordes 1998a, 1998b). Finally, the recent completion of the Wisconsin Hα Mapper (WHAM) survey of diffuse Galactic Hα emission with 1° angular resolution and ~ 10 km s^{-1} velocity resolution (Reynolds et al. 1998; Haffner 2000) will allow the development of more complex models. These observations will allow for a reassessment of the location of Galactic spiral arms (Georgelin & Georgelin 1976; Russeil et al. 1998; Georgelin et al. 2000), as well as the discovery and placement of large angular scale H II regions, such as the Gum Nebula.

In this work, we present an updated list of pulsars of known distance. We then use these data to constrain a new axisymmetric model for the free electron distribution and show how the Taylor-Cordes model and the new axisymmetric model fare in predicting distances to the pulsars. We also consider to what degree the available data constrain the lumpiness of the WIM. Incorporation of nonaxisymmetric effects, such as the Galactic spiral arms and individual nebulae, can subsequently be incorporated using the WHAM data and more recent radio recombination line surveys of H II regions.

2. THE PULSAR DATA SET

A list of 109 pulsars with distance information was gathered from a number of sources, and this information is compiled in Table 1, presented in order of increasing distance. Of this list, four are in the Large or Small Magellanic Cloud. Of the remainder, 76 have both upper and lower distance limits; 20 have only lower limits, and nine have only upper limits. This data set is $\sim 50\%$ larger than the data used by TC. Of the 109 pulsars, there are 35 new distance determinations since the compilation of Frail & Weisberg (1990, hereafter FW90), which provided the bulk of the measurements used in the TC model, 25 objects for which there have been revisions in either the distance or the

[1] Also Department of Astronomy, University of Wisconsin–Madison, 475 North Charter Street, Madison, WI 53706.

TABLE 1

PULSARS WITH INDEPENDENT DISTANCE INFORMATION

PSR	l (deg)	b (deg)	DM (cm^{-3} pc)	D_{min} (kpc)	D (kpc)	D_{max} (kpc)	$\langle n_e \rangle$ (10^{-3} cm^{-3})	Method[a]	Refs.
0435−47[b]	253.40	−42.00	2.60	0.16	0.18	0.21	14.4	PDD	1
0656+14[b]	201.11	8.26	14.02	0.12	0.18	0.23	77.9	X	2
1929+10[c]........	47.38	−3.88	3.18	0.15	0.20	0.29	15.9	**Π**, K	3, 4, 5, **6**
0833−45[c]........	263.55	−2.79	68.20	0.22	0.25	0.28	272.8	**Vela SNR**, Π	7, **8**
0950+08[c]........	228.90	43.70	3.00	0.25	0.28	0.31	10.7	Π	9, **10**
1741−11[b]	14.79	9.18	3.14	0.33	0.36	0.39	8.7	TP	11
0823+26	197.00	31.70	19.50	0.29	0.36	0.45	54.2	Π	9
1451−68	313.90	−8.50	8.60	0.40	0.45	0.53	19.1	Π	12
1855+09[c]........	42.29	3.06	13.31	0.71	0.91	1.25	14.6	**TP**, K	13, **14**
2021+51[b]	87.86	8.38	22.58	0.76	1.05	1.72	21.5	Π	15
1534+12[b]	20.00	47.80	11.62	0.93	1.08	1.23	10.8	PDD, TP	16
1259−63[b]	304.2	−0.992	146.72	0.60	1.10	1.60	133.4	SP	17
1711+07[b]	28.75	25.22	15.99	0.83	1.11	1.67	14.4	TP	18
0919+06[b]	225.42	36.39	27.31	1.04	1.20	1.43	22.7	Π	**19**, 20
0355+54	148.20	0.80	57.00	1.40	1.80	2.20	31.7	K	21, 22, 23
0329+54	145.00	−1.20	26.80	1.70	1.85	2.00	14.5	K	23, 24, 25, 26, 27
0531+21	184.56	−5.78	56.79	1.50	2.00	2.50	28.4	Crab SNR	28
1358−63[b]	310.60	−2.10	98.00	1.60	2.15	2.70	45.6	K	29
1620−26[c]........	350.98	15.96	62.86	1.97	2.20	2.46	28.6	NGC 6121 (M4)	30, 31
1740−53[b]	338.20	−11.90	71.80	2.12	2.30	2.49	31.2	NGC 6397	30, 32, 33
1951+32	68.77	2.82	44.98	1.00	2.50	4.00	18.0	CTB 80 SNR	34
1807−24[b]	5.80	−2.20	134.00	2.17	2.60	3.11	51.5	NGC 6544	30, 32, 35
1054−62[c]........	290.30	−3.00	321.00	2.50	2.70	2.90	118.9	K	36, 37, **38**
0138+59	129.10	−2.10	34.80	2.60	2.75	2.90	12.7	K	22
1706−44[b]	343.10	−2.70	76.00	2.40	2.80	3.20	27.1	K	38
1853+01	34.56	−0.50	96.70	2.70	3.30	3.90	29.3	W44 SNR	39
1900+01	35.70	−2.00	246.40	2.80	3.40	4.00	72.5	K	40
2334+61[b]	114.28	0.23	58.38	3.00	3.40	3.80	17.2	G114.3+0.3 SNR	41
1900+05	39.50	0.20	179.70	3.10	3.70	4.30	48.6	K	27
1859+07	40.60	1.10	261.00	2.80	3.75	4.70	69.6	K	42
0835−41[c]........	260.90	−0.30	148.00	1.80	3.90	6.00	37.9	K	**29**, 43
1910−59[b]	336.5	−25.60	34.00	3.79	4.00	4.22	8.5	NGC 6752	30, 32, 44
1046−58[b]	287.40	0.60	129.00	2.50	4.05	5.60	31.9	K	29
1509−58	320.32	−1.16	253.20	3.50	4.40	5.30	57.5	MSH 15−52 SNR	39
1800−21	8.40	0.10	234.20	4.00	4.45	4.90	52.6	K, G8.7−0.1 SNR	27, 45
0740−28[c]........	243.80	−2.40	74.00	2.00	4.45	6.90	16.6	K	26, **38**, 46
0021−72C[c]......	305.92	−44.89	24.61	4.27	4.50	4.75	5.5	NGC 104 (47 Tuc)	30, 47
1845−01	31.30	0.00	159.10	4.20	4.50	4.80	35.3	K	36, 48
0906−49[b]	270.30	−1.00	181.00	2.40	4.55	6.70	39.8	K	38
1641−45	339.20	−0.20	475.00	4.20	4.60	5.00	103.3	K	27, 49
1830−08[b]	23.40	0.10	411.00	4.00	4.65	5.30	88.4	K	50
1718−35[b]	351.70	0.70	496.00	4.40	4.80	5.20	103.3	K	50
1914+13	47.60	0.50	236.80	4.00	4.85	5.70	48.8	K	48
1907+10	44.80	1.00	148.40	4.30	5.15	6.00	28.8	K	48
1758−23[b]	6.80	−0.10	1074.00	3.50	5.20	6.90	206.5	K, W28 SNR	51
1829−08	23.30	0.30	300.00	4.70	5.25	5.80	57.1	K	27
1915+13	48.30	0.60	94.80	4.80	5.25	5.70	18.1	K	48
2111+46	89.00	−1.30	141.50	4.30	5.40	6.50	26.2	K	22
1821−24[c]........	7.80	−5.58	119.83	5.03	5.70	6.46	21.0	NGC 6626 (M28)	30, 52
1154−62[b]	296.70	−0.20	325.00	3.80	6.40	9.00	50.8	K	29
1701−30[b]	353.60	7.30	114.40	6.04	6.90	7.88	16.6	NGC 6266 (M62)	30, 32, 53
1338−62[b]	308.73	−0.04	730.00	4.00	6.90	9.80	105.8	G308.8−0.1 SNR	54
1908+00[c]........	35.54	−4.71	201.50	6.13	7.40	8.93	27.2	NGC 6760	30, 55
1516+02B[c]......	3.86	46.80	30.50	7.12	7.50	7.90	4.1	NGC 5904 (M5)	30, 56
1744−24A[c]......	3.84	1.70	242.14	4.69	7.60	12.31	31.9	Terzan 5	30, 57
1639+36A[c]......	59.00	40.91	30.36	7.33	7.70	8.09	3.9	NGC 6205 (M13)	30, 58
1221−63[b]	300.00	−1.40	97.00	4.30	7.85	11.4	12.4	K	29
1820−30A[c]......	2.79	−7.91	86.80	7.26	8.00	8.82	10.9	NGC 6624	30, 59
1240−64	302.10	−1.50	297.40	4.50	8.00	11.5	37.2	K	37, 49
1802−07[c]........	20.79	6.77	186.38	6.71	8.40	10.52	22.2	NGC 6539	30, 60
1745−20[c]........	7.73	3.80	220.00	6.59	8.40	10.71	26.2	NGC 6440	30, 61
1558−50[c]........	330.70	1.30	169.50	7.40	8.40	9.40	20.2	K	48, 62
1323−62	307.10	0.20	318.40	5.10	8.45	11.8	37.7	K	49
1718−19[c]........	4.87	9.74	71.00	7.55	8.60	9.80	8.3	NGC 6342	30, 55

TABLE 1—*Continued*

PSR	l (deg)	b (deg)	DM (cm^{-3} pc)	D_{min} (kpc)	D (kpc)	D_{max} (kpc)	$\langle n_e \rangle$ (10^{-3} cm^{-3})	Method[a]	Refs.
2002+31	69.00	0.00	234.70	7.00	9.50	12.0	24.7	K	40
1937+21	57.51	−0.29	71.04	4.60	9.70	14.8	7.3	**K**, TP	14, 63
1929+20	55.60	0.60	211.00	4.80	9.85	14.9	21.4	K	27
1904+06	40.60	−0.30	473.00	6.50	10.25	14.0	46.1	K	42
1913+10	44.70	−0.70	246.10	6.00	10.25	14.5	24.0	K	27
2127+11A[c]......	65.01	−27.31	67.31	9.66	10.30	10.99	6.5	NGC 7078 (M15)	30, 64
1859+03	37.20	−0.60	402.90	6.80	10.95	15.1	36.8	K	40, 49
1900+06	39.90	0.40	530.00	6.50	11.15	15.8	47.5	K	27
1849+00	33.50	0.00	680.00	7.10	11.85	16.6	57.4	K	42
1930+22	57.40	1.60	211.30	10.40	12.05	13.7	17.5	K	27
1557−50[c]........	330.70	1.60	270.00	6.40	12.30	18.2	22.0	K	36, 49, 62
1310+18[c]........	332.96	79.77	24.00	17.41	18.30	19.23	1.3	NGC 5024 (M53)	30, 65
0456−69	281.20	−35.19	91.00	46.00	49.40	52.8	1.8	LMC	66
0502−66	277.03	−35.50	65.00	46.00	49.40	52.8	1.3	LMC?	66
0529−66	277.02	−32.80	100.00	46.00	49.40	52.8	2.0	LMC	66
0042−73	303.51	−43.80	105.40	52.80	57.00	61.2	1.8	SMC	66
1749−28	1.50	−1.00	50.90	0.13	...	...	<391.5	K	25
1857−26[b]	10.34	−13.45	38.06	0.91	...	...	<41.8	Π	20
1804−08	20.10	5.60	112.80	1.50	...	...	<75.2	K	27
1821+05	35.00	8.90	67.50	1.60	...	...	<42.2	K	27, 42, 48
1920+21	55.30	2.90	217.10	1.90	...	...	<114.3	K	48
1556−44[b]	334.50	6.40	59.00	2.00	...	...	<29.5	K	38
0736−40[c]........	254.20	−9.20	161.00	2.10	...	...	<76.7	K	26, 29, 49, 67
1449−64[b]	315.70	−4.40	71.00	2.50	...	...	<28.4	K	38
2319+60	112.10	−0.60	93.80	2.60	...	...	<36.1	K	21, 22, 23
1323−58[b]	307.50	3.60	286.0	3.00	...	...	<95.3	K	68
2020+28	68.90	−4.70	24.60	3.10	...	...	<7.9	K	5, 21, 22
2016+28	68.10	−4.00	14.20	3.20	...	...	<4.4	K	5, 26, 42, 69
1821−19[b]	12.30	−3.10	224.30	3.20	...	...	<70.1	K	62
2255+58	108.80	−0.60	151.10	3.30	...	...	<45.8	K	27
1757−24[b]	5.26	−0.88	289.00	3.50	...	...	<82.6	G5.4−1.2 SNR	70
1703−40[b]	345.70	−0.20	360.00	3.80	...	...	<94.7	K	50
1648−42[b]	342.50	0.90	525.00	4.80	...	...	<109.4	K	50
1933+16	52.40	−2.10	158.50	5.20	...	...	<30.5	K	3, 23, 26, 71
1356−60	311.20	1.10	295.00	5.60	...	...	<52.7	K	36
1855+02	35.60	−0.40	506.00	6.90	...	...	<73.3	K	42
1818−04	25.50	4.70	84.40	...	...	1.60	>52.8	K	46
1822−09	21.40	1.30	19.90	...	...	1.90	>10.5	K	21, 62
1944+17	55.30	−3.50	16.30	...	...	1.90	>8.6	K	48
1919+21	55.80	3.50	12.40	...	...	2.80	>4.4	K	5
1737−30[b]	358.30	0.20	153.00	...	...	5.50	>27.8	K	62
1742−30[b]	358.60	−1.00	88.80	...	...	5.50	>16.2	K	62
0959−54[c]........	280.20	0.10	131.00	...	...	6.90	>19.0	K	36, 38
0940−55[b]	278.60	−2.20	180.00	...	...	7.50	>24.0	K	29
0905−51[b]	272.2	−3.0	104.00	...	...	8.00	>13.0	K	68

[a] Methods of determining the pulsar distances are (K) kinematic; (Π) trigonometric parallax; (T) timing parallax; (X) X-ray luminosity model; (SP) spectroscopic parallax of binary companion; (PDD) period-derivative distance; and association with SNRs of known distance, globular clusters, or the Large or Small Magellanic Cloud. In the cases where more than one method was used, we note in boldface which method (and reference) we chose for the tabulated distance.

[b] New pulsar distance determination since Frail & Weisberg 1990.

[c] Revised distance estimate since Frail & Weisberg 1990.

REFERENCES.—(1) Sandhu et al. 1997; (2) Golden & Shearer 1999; (3) Gordon & Gordon 1970; (4) Gómez-González et al. 1972, Salter et al. 1979, Backer & Sramek 1982; (5) Weisberg, Rankin, & Boriakoff 1980; (6) Campbell 1995; (7) Cha et al. 1999; (8) Legge 2000; (9) Gwinn et al. 1986; (10) Brisken et al. 2000; (11) Toscano et al. 1999; (12) Bailes et al. 1990; (13) Kulkarni et al. 1991, Ryba & Taylor 1991; (14) Kaspi et al. 1994; (15) Campbell et al. 1996; (16) Stairs et al. 2000; (17) Johnston et al. 1994; (18) Camilo, Foster, & Wolszczan 1994; (19) Chatterjee et al. 2001; (20) Fomalont et al. 1999; (21) Gómez-González & Guélin 1974; (22) Graham et al. 1974; (23) Booth & Lyne 1976; (24) de Jager et al. 1968; (25)Guélin et al. 1969, Gordon, Gordon, & Shalloway 1969; (26) Gordon & Gordon 1973; (27) Frail et al. 1991; (28) Trimble & Woltjer 1971; (29) Johnston et al. 1996; (30) Harris 1996 and updates at http://physun.mcmaster.ca/Globular.html; (31) Cudworth & Rees 1990; (32) D'Amico et al. 2001; (33) Alcaino et al. 1987; (34) Blair et al. 1984; (35) Alcaino 1983; (36) Manchester, Wellington, & McCulloch 1981; (37) Frail & Weisberg 1990; (38) Koribalski et al. 1995; (39) Caswell et al. 1975; (40) Weisberg, Boriakoff, & Rankin 1979; (41) Fesen et al. 1997; (42) Clifton et al. 1988; (43) Gordon & Gordon 1975; (44) Buonanno et al. 1986; (45) Finley & Ögelman 1994; (46) Gómez-González et al. 1973; (47) Hesser et al. 1987; (48) Weisberg et al. 1987; (49) Ables & Manchester 1976; (50) Weisberg et al. 1995; (51) Frail et al. 1993; (52) Rees & Cudworth 1991; (53) Brocato et al. 1996a; (54) Caswell et al. 1992; (55) Heitsch & Richtler 1999; (56) Brocato, Castellani, & Ripepi 1996b, Sandquist et al. 1996; (57) Ortolani, Barbuy, & Bica 1996; (58) Paltrinieri et al. 1998; (59) Sarajedini & Norris 1994; (60) Armandroff 1988; (61) Ortolani, Barbuy, & Bica 1994; (62) Johnston et al. 2001; (63) Heiles et al. 1983; (64) Durrell & Harris 1993; (65) Rey et al. 1998; (66) Feast & Walker 1987; (67) Manchester, Murray, & Radhakrishnan 1969; (68) Saravanan et al. 1996; (69) Encrenaz & Guélin 1970; (70) Caswell et al. 1987; (71) Guélin, Encrenaz, & Bonazzola 1971.

distance uncertainty of the pulsar, and 49 objects whose distance estimates remain unchanged.

The distance estimates come from a variety of methods, which we briefly summarize here.

Kinematic distances (*68 pulsars*).—The majority of pulsar distance measurements come from the combination of 21 cm absorption combined with an axisymmetric, kinematic model for Galactic rotation (Fich, Blitz, & Stark 1989). FW90 reevaluated all the distance measurements up to that time using this model (with corrections for pulsars toward the Perseus arm) and a uniform set of criteria for converting absorption velocities to distance. These criteria have been adhered to in subsequent work. Probably the largest source of systematic error is due to the noncircular "streaming" motions in the vicinity of spiral arms.

Association with globular clusters (*17 pulsars*).—The next most common method of distance determination comes from association of a pulsar with a globular cluster of known distance. Table 1 only lists one pulsar per globular cluster; when more than one pulsar is known, the variation in dispersion measure is small. Since the compilation of FW90, the distances to globular clusters have been considerably refined as a result of improved color-magnitude diagrams and shifts in the assumptions about the luminosity of RR Lyrae stars. As a result, some distance estimates have been revised by more than a factor of 2 since FW90 (Harris 1996).[2] The uncertainty in the distance moduli of these clusters was assumed to be $\sigma = 0.1 + 0.4E_{B-V}$ mag. More heavily reddened clusters have poorer data, since they present greater problems with field contamination and crowding (W. E. Harris 1999, private communication).

Association with supernova remnants (*10 pulsars*).—There have been numerous suggested associations between pulsars and supernova remnants (Lorimer, Lyne, & Camilo 1998; Gaensler & Johnston 1995; Frail, Goss, & Whiteoak 1994; Kaspi et al. 1996). However, such associations are hard to prove, since they depend upon expectations for supernova remnant (SNR) lifetimes, pulsar ages, and transverse velocities. In this compilation, we use the associations judged by Lorimer et al. (1998) to be the "most likely" pulsar–SNR pairs. The only other pulsar-SNR associations added were B1800−21 with G8.7−0.1 (Finley & Ögelman 1994) and B1758−23 with W28 (Frail, Kulkarni, & Vasisht 1993). Both of these have independent kinematic distances that support the association.

Trigonometric parallax (*8 pulsars*).—Potentially the most reliable distances come from interferometric measurements of annual parallax. However, there are several practical difficulties arising from ionospheric effects and a scarcity of nearby calibrators for positions. Improvements in the techniques have led to changes in the published distances by more than a factor of 2. The distance estimate for B0950+08 increased from 130 pc (Gwinn et al. 1986) to 280 pc (Brisken et al. 2000), while the distance estimate for B0919+06 decreased from 3.3 kpc (Fomalont et al. 1999) to 1.2 kpc (Chatterjee et al. 2001). These changes were much larger than the stated uncertainties in the measurements. Accurate estimates are vital if pulsars are to be used as probes of the structure of the local interstellar medium.

Association with other galaxies (*4 pulsars*).—Four pulsars have been associated with the Magellanic Clouds, three in the LMC and one in the SMC. These pulsars are valuable in constraining the electron density in the Galactic halo. However, an unknown fraction of the dispersion measure must arise in the host galaxy, so their utility in constraining the Galactic free electron column density is compromised.

Timing parallax (*5 pulsars*).—Distances to millisecond pulsars have also been estimated using variations in the arrival times of the pulses. There is a annual change in the pulse arrival time whose magnitude is given by $\Delta t = r^2 \cos^2 \theta/(2cd)$, where r is the Earth-Sun distance, θ is the angle between the line of sight and the ecliptic plane, and d is the distance (Ryba & Taylor 1991). This variation is $\Delta t = 1.2$ μs for $d = 1$ kpc. This level of timing accuracy has been reached for only a few pulsars.

Period-derivative distances (*2 pulsars*).—Bell & Bailes (1996) have shown that in many cases, the observed orbital period derivative of binary pulsars is dominated by a term of the form $\dot{P}_b/P_b = v^2/(cd)$. If one uses the predictions of general relativity to derive the intrinsic period derivative, knowledge of the proper motion of the pulsar then allows for an accurate estimate of the distance. This method has been applied to only two pulsars to date.

Spectroscopic parallax of binary companion (*1 pulsar*).—There is one case in which the binary companion of a pulsar is a $\sim 10\ M_\odot$ Be star (Johnston et al. 1994). In this case, spectroscopic parallax was used to estimate the distance.

X-ray luminosity distance (*1 pulsar*).—There is one distance estimate for B0656+14 based upon the identification of the X-ray counterpart used together with a model of thermal X-ray emission from the neutron star (Golden & Shearer 1999). As will be seen, this pulsar ends up being an outlier in our model. As a result, we are not convinced that this method is reliable.

Trigonometric parallax of optical counterpart (*0 pulsars*).—If the optical counterpart of a pulsar can be identified, then ground-based or *Hubble Space Telescope* observations could yield a parallax estimate. This technique has been used to determine the distance to the neutron star Geminga (Caraveo et al. 1996). However, we have not included Geminga in our list, because it is unclear whether it has a reliable radio signal. The search for optical counterparts of pulsars has been relatively unsuccessful to date (Caraveo 2000). Still, we think this method holds some promise, particular for pulsars with the very lowest dispersion measures, such as J0108−1431, which has DM = 1.83 cm^{-3} pc (Tauris et al. 1994).

Scattering-screen distance (*0 pulsars*).—It has been suggested that the transverse velocity of a pulsar derived using models of interstellar scintillation can be combined with measurements of proper motion to constrain the distance to the pulsar (Gupta 1995; Deshpande & Ramachandran 1998; Cordes & Rickett 1998). Application of this model requires a knowledge of the distribution of electron density and scattering properties along the line of sight and, as a result, is principally useful for pulsars that lie behind H II regions of known distance or pulsars well above the disk of the Galaxy.

Cross-checks (*7 pulsars*).—There are seven pulsars for which two independent methods have been applied for distance determination. In each case, the distance estimates agree within the stated errors, although in two cases the agreement is marginal. Such checks are important, since

[2] With on-line updates at http://physun.mcmaster.ca/Globular.html.

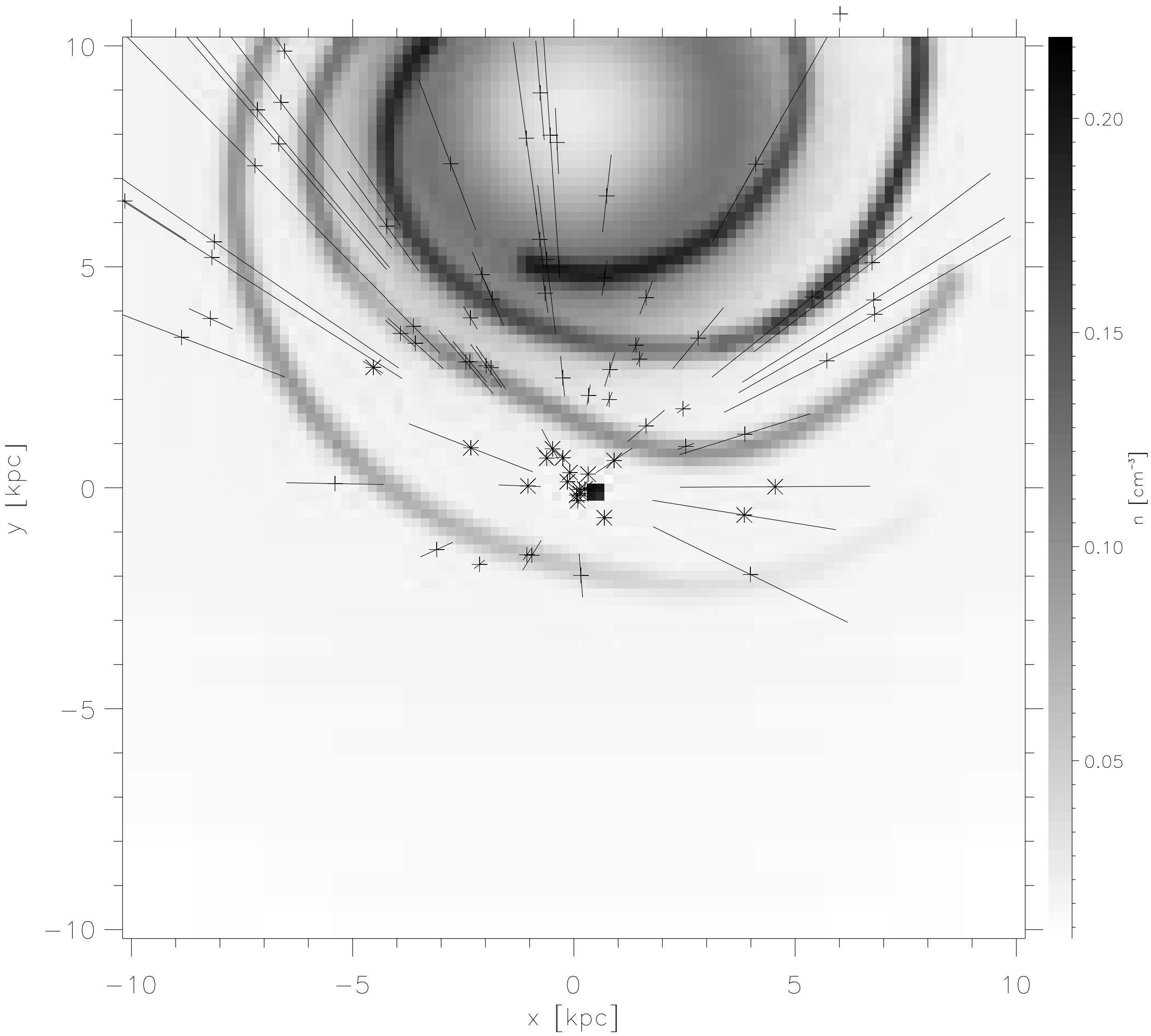

FIG. 1.—Projection of the positions of the pulsars onto the Galactic plane. Uncertainties in the distance from the Sun are also shown. The location and density of the spiral arms, central annulus, and Gum Nebula in the Taylor-Cordes model are noted in gray scale. Pulsars marked with a star are those considered to be in the "interarm direction" as seen from the Sun, although this neglects the potential contribution of the Local arm.

they test the reliability of the individual methods. We summarize these results here.

B1929+10: This pulsar has three discrepant measures for trigonometric parallax, $\pi = 21.5 \pm 0.3$ mas (Salter, Lyne, & Anderson 1979), $\pi < 4$ mas (Backer & Sramek 1982), and $\pi = 5.0 \pm 1.5$ mas (Campbell 1995). The kinematic distance is $d < 1.6$ kpc (Weisberg, Rankin, & Boriakoff 1987). We have adopted the most recent parallax distance, which is consistent with the kinematic distance.

B0833−45: The distance to the Vela SNR is given as $d = 250 \pm 30$ pc (Cha, Sembach, & Danks 1999), while recent VLBI parallax gives $d = 316^{+37}_{-29}$ pc (Legge 2000). While these uncertainties do not overlap, the uncertainties in stellar distances may be slightly underestimated.

B1855+09: The timing-parallax distance to this pulsar was given as $d = 0.83^{+0.66}_{-0.24}$ pc (Ryba & Taylor 1991), later refined to $d = 0.91^{+0.34}_{-0.20}$ pc (Kaspi, Taylor, & Ryba 1994). This agrees marginally well with the kinematic distance limits $d_{\rm lower} = 1.6 \pm 0.5$ to $d_{\rm upper} = 2.0 \pm 0.4$ (Kulkarni, Djorgovski, & Klemola 1991).

B1800−21: The kinematic distance limits to this pulsar are $d_{\rm lower} = 4.0 \pm 0.6$ kpc and $d_{\rm upper} = 4.9 \pm 0.3$ kpc, which agree with the kinematic distance to the SNR G8.7−0.1, also established kinematically (Finley & Ögelman 1994).

B1758−23: The kinematic distance limits to this pulsar are $d_{\rm lower} = 3.5 \pm 0.9$ kpc and $d_{\rm upper} = 6.9 \pm 0.1$ kpc, which agree with the kinematic distance to W28, also established kinematically (Frail et al. 1993).

B1937−21: The kinematic distance limits are $d_{\rm lower} = 4.6 \pm 1.9$ kpc and $d_{\rm upper} = 14.8 \pm 0.9$ kpc (Heiles et al. 1983), which agree with the timing-parallax distance of $d > 3.6$ kpc (Kaspi et al. 1994).

B1534+12: The period-derivative distance to this binary pulsar is $d = 1.08 \pm 0.15$ kpc, which is consistent with the timing-parallax limit of $d > 0.67$ kpc (Stairs et al. 2000).

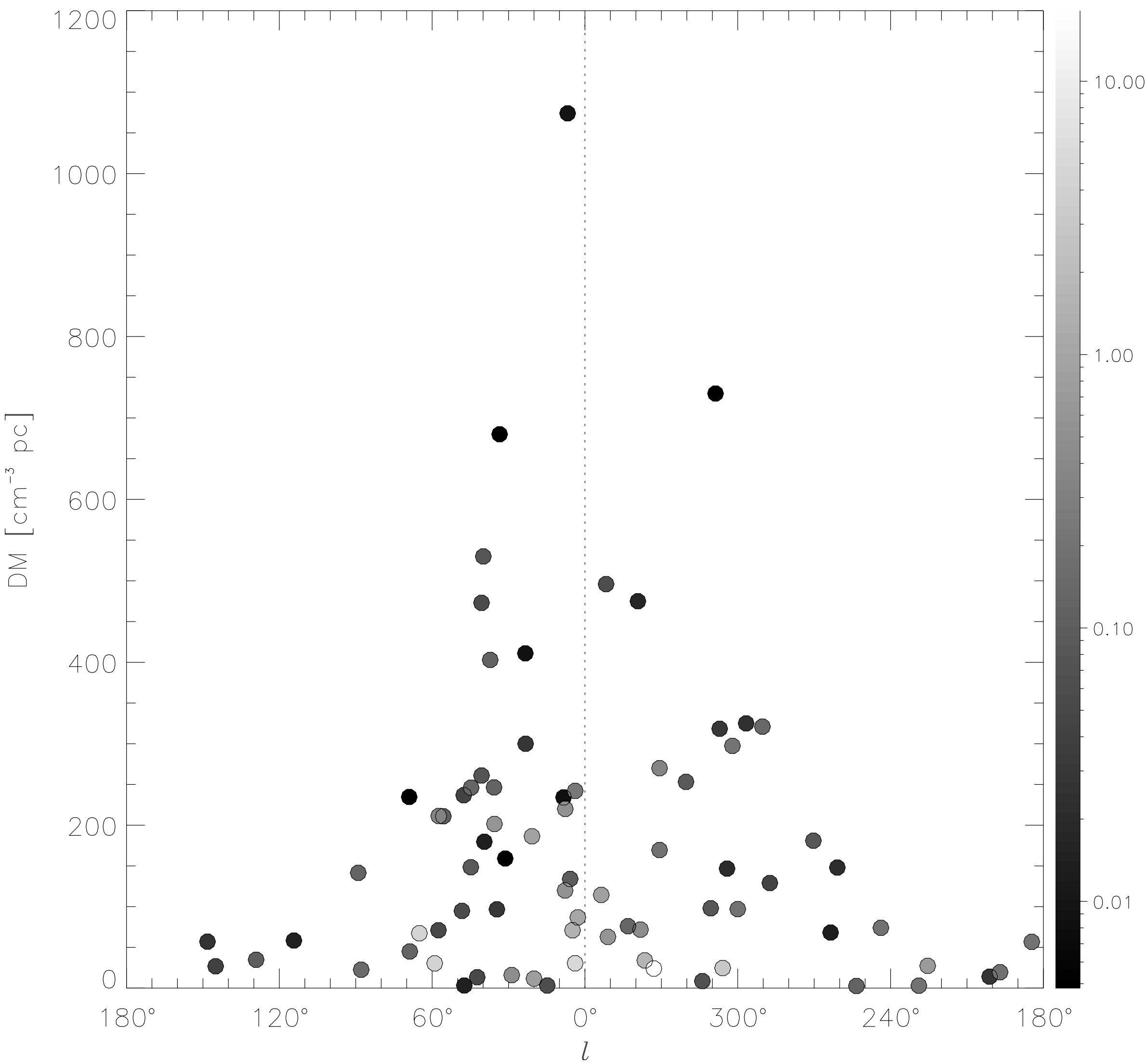

FIG. 2.—Distribution of pulsar dispersion measure with Galactic longitude. The gray scale indicates distance from the Galactic midplane. In this data set, there is no clear evidence for an asymmetric distribution with Galactic longitude.

Figure 1 shows the spatial distribution of the pulsars in our sample with both upper and lower distance limits projected onto the Galactic plane, while Figure 2 shows a plot of their dispersion measure as a function of Galactic longitude. Note that in Figure 2 there is no clear evidence of the asymmetry in maximum dispersion measure around $l = 0°$, which is present in the complete set of pulsars including those of unknown distance.

3. FITTING AN AXISYMMETRIC MODEL

Using this information, we fitted a two-component model of the Galactic disk to the pulsar data. The model has the form

$$n_e(r, z) = n_0 \frac{f(r/r_0)}{f(r_\odot/r_0)} f\left(\frac{z}{z_0}\right) + n_1 \frac{f(r/r_1)}{f(r_\odot/r_1)} f\left(\frac{z}{z_1}\right),$$

where $f(x)$ is either $\exp(-x)$ or $\mathrm{sech}^2\, x$ and $r_\odot = 8.5$ kpc is the Galactocentric distance of the Sun. The fit was achieved through a variant of the χ^2 method: We defined the error of the fit Δ as

$$\Delta = \frac{1}{n - v} \sum \frac{\log^2 (\mathrm{DM_{data}}/\mathrm{DM_{model}})}{\sigma^2 + \sigma_A^2},$$

where n is the number of pulsars (76) with both upper and lower distance limits, v is the number of free parameters in the model (six), $\mathrm{DM_{data}}$ are the observed dispersion measures, $\mathrm{DM_{model}}$ are the modeled dispersion measures, obtained by integrating the model through the line of sight to each pulsar position, $\sigma = 0.5 \log(D_{\max}/D_{\min})$ with $D_{\max}$ and $D_{\min}$ the 1 σ distance brackets, $\sigma_A = 0.5 \log[(1 + A)/(1 - A)]$, and A is a noise parameter. The form of this extra term comes from assuming that there is extra error proportional to the dispersion measure, i.e.,

$$\mathrm{DM}_A = \mathrm{DM_{model}}(1 \pm A),$$

$$\sigma_A = 0.5 \log(\mathrm{DM}_{A+}/\mathrm{DM}_{A-}).$$

Most of the distances to the pulsars we used (41 out of 76) were determined by assuming a kinematic model for the

Galactic rotation and comparing it with the 21 cm absorption observed toward the pulsar. For these pulsars, we define the distance to be halfway between the minimum and maximum limits. For these distances, there is a uniform probability for the location of the pulsar between the distance brackets, as opposed to the distances obtained by parallaxes, for example, which have a Gaussian probability distribution for the distance around a preferred value. Therefore, the kinematic distances have an extra factor of $1/\sqrt{3}$ in the corresponding σ.

An annealing procedure was used to obtain the best fit for the parameters n_0, n_1, r_0, r_1, z_0, and z_1 with $A = 0$. Then A was adjusted to yield $\Delta = 1$ and a new fit was obtained. The procedure was repeated until convergence was achieved. Outlying pulsars were spotted by a procedure described below, and those common to both functional forms were taken out of the sample. Then the procedure was repeated, and the new fit was considered final. The parameters of the best fits are listed in Table 2. The results of the fit for the $f(x) = \mathrm{sech}^2\, x$ case are presented in Figure 3. The corresponding density profiles are shown in Figure 4. There are not enough data to distinguish between the two functional forms, but the resulting fit parameters are different in each case. We prefer the $\mathrm{sech}^2\, x$ model because it does not have a midplane cusp and yields fewer outliers. For this

TABLE 2

BEST-FIT PARAMETERS

Model	$n(r = r_\odot, z = 0)$ (cm^{-3})	z (kpc)	r (kpc)	A
$\mathrm{sech}^2\, x$	1.77×10^{-2}	1.10	15.4	0.30
	1.07×10^{-2}	0.04	3.6	
$\exp(-x)$	2.03×10^{-2}	1.07	30.4	0.31
	0.71×10^{-2}	0.05	1.5	

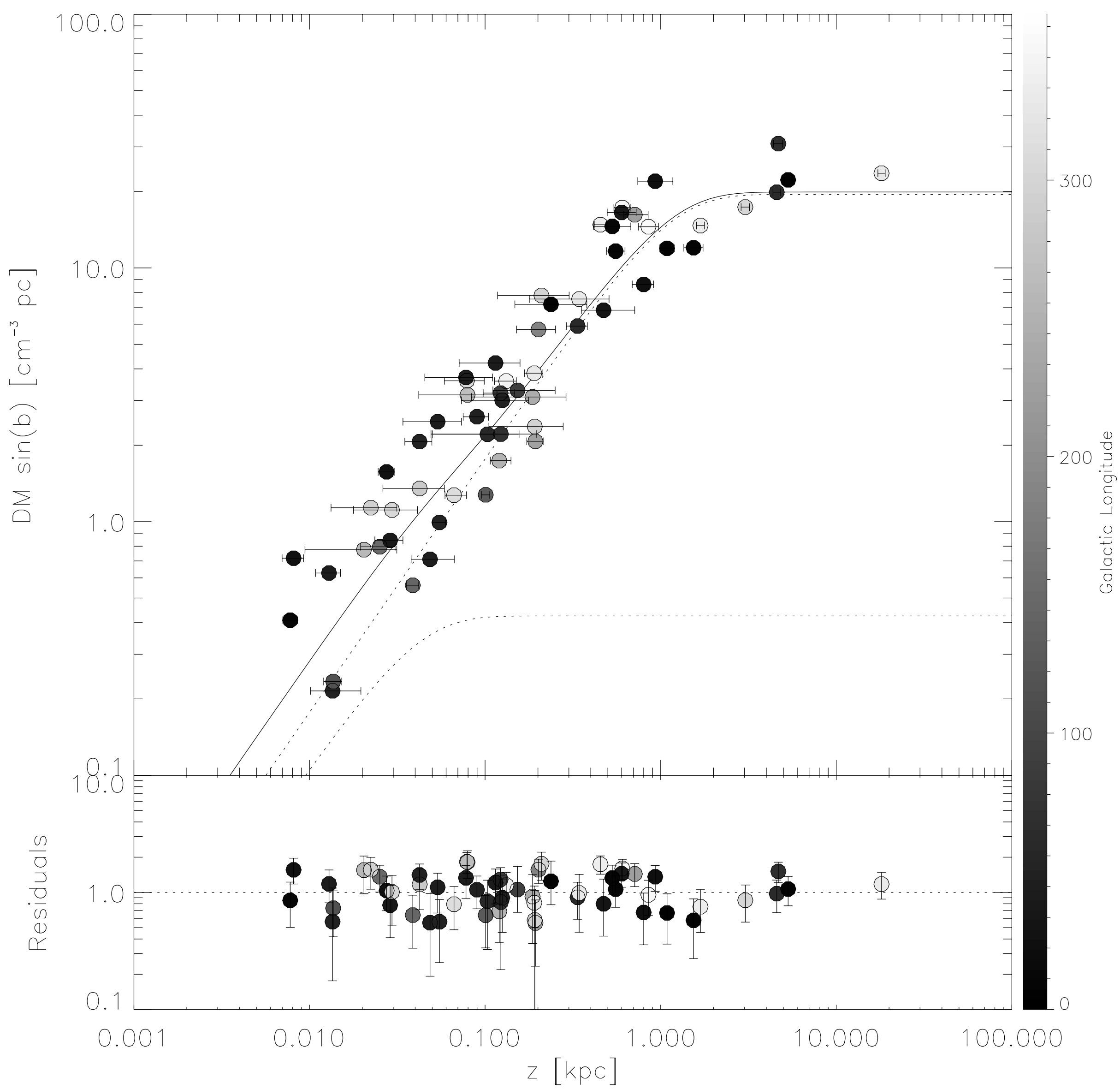

FIG. 3.—*Top*: DM sin b as a function of z for the pulsars used in fitting our final model. The solid line shows the two-component model with $f(x) = \mathrm{sech}^2\, x$ at the solar radius. The dotted lines show the individual components. The error bars show only the effects of distance uncertainty and do not incorporate the noise parameter. *Bottom*: The residual values for our fit, defined as $\mathrm{DM_{data}/DM_{model}}$. The uncertainties incorporate the effects of our noise parameter, $A = 0.30$. No clear trend in the residuals with Galactic longitude (*gray scale*) is observed.

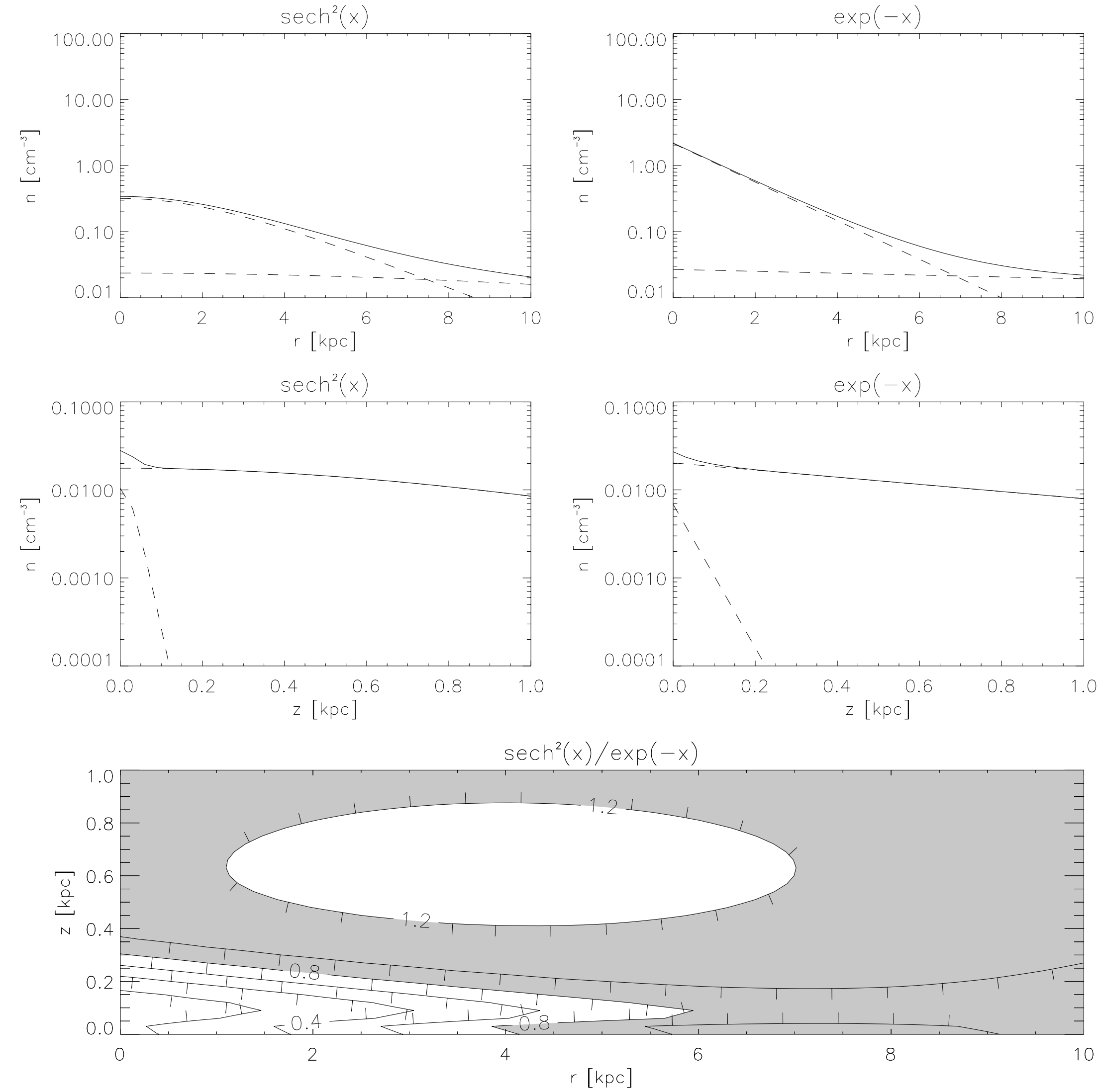

FIG. 4.—Resulting density distributions and comparison of the two functional forms. Dashed lines show the individual components, and the solid lines show the sum. *Top*, midplane density vs. Galactocentric radius; *middle*, $n(z)$ for $r = r_\odot = 8.5$ kpc; *bottom*, the ratio of the two model densities vs. r and z. The pulsar data set does not allow us to distinguish between the two functional forms. The shaded region shows where the predicted electron densities from the two models differ by less than 20%.

case,

$$
\begin{aligned}
n_e(r, z) = {} & (1.77 \times 10^{-2}\ \mathrm{cm}^{-3}) \\
& \times \frac{\mathrm{sech}^2\,[r/(15.4\ \mathrm{kpc})]}{\mathrm{sech}^2\,[r_\odot/(15.4\ \mathrm{kpc})]}\,\mathrm{sech}^2\left(\frac{z}{1.10\ \mathrm{kpc}}\right) \\
& + (1.07 \times 10^{-2}\ \mathrm{cm}^{-3}) \\
& \times \frac{\mathrm{sech}^2\,[r/(3.6\ \mathrm{kpc})]}{\mathrm{sech}^2\,[r_\odot/(3.6\ \mathrm{kpc})]}\,\mathrm{sech}^2\left(\frac{z}{0.04\ \mathrm{kpc}}\right) .
\end{aligned}
$$

These results are comparable to the previous axisymmetric model of Cordes et al. (1991), although our thin disk component has a lower midplane density ($n = 10^{-2}$ cm^{-3} vs. $n = 20 \times 10^{-2}$ cm^{-3}) and a shorter scale height ($h = 40$ pc vs. $h = 175$ pc). We also find a noise parameter of $A = 0.30$. Savage, Edgar, & Diplas (1990) performed a similar study with a smaller sample of pulsars. The value of the exponential scale height found is consistent with theirs within the error bars, but their intrinsic scatter ($1.65 = 1 + A$) is larger than ours.

The procedure for spotting the outliers was as follows: Consider the values of $\mathrm{DM_{model}}$ obtained by integrating n_e in the line of sight toward each pulsar to the distance brackets, and call them DM_+ and DM_-. Now consider the values

$$
x_\pm = \frac{\mathrm{DM_{data}}}{\mathrm{DM_{model}}} \pm \sqrt{\left(\frac{\mathrm{DM_{model}} - \mathrm{DM}_\pm}{\mathrm{DM_{model}}}\right)^2 + A^2}
$$

for each pulsar (the error bars in the bottom panel of Fig. 3 are the values of the square root above). If $\mathrm{sgn}\,(x_+ - 1) = \mathrm{sgn}\,(x_- - 1)$, then that pulsar is considered an outlier. As mentioned above, the pulsars spotted as outliers for both functional forms were taken out of the sample for the final calculation of the fit.

4. DEVIATIONS FROM THE SMOOTH AXISYMMETRIC MODEL

Since observations of H II regions in the Galaxy show that there are clearly inhomogeneities and asymmetries in the distribution of free electrons, we have looked for patterns in the spatial and statistical distribution of our residuals, DM_{data}/DM_{model}. We discuss in turn the individual outliers, the distribution of residuals with respect to longitude and distance, and the nature of the scatter about our smooth model. In the future, the combination of these data with new radio recombination surveys for distant H II regions and velocity-resolved Hα surveys of more nearby gas will yield a more complicated, but realistic, model.

4.1. *Outliers*

Of the 76 pulsars with both upper and lower limits, 15 are outliers in both the exponential and $\mathrm{sech}^2 x$ models. These outliers are noted in Table 3, together with the observed dispersion measure and the dispersion measure that we would predict given the distance, $DM_{\pm} = (1 \pm A)DM_{model}(D)$. Two of these pulsars have dispersion measures that are lower than one would expect given their distance. The first, B1741−11, with a timing-parallax distance, is only 0.36 kpc away. Given the lumpiness of the local interstellar medium (Cox & Reynolds 1987; Toscano et al. 1999), it is not out of the question for such a low-density sight line to arise for such a short distance. The second pulsar with a much lower dispersion measure than expected is B1937+21. This object, which has a kinematic distance of $d = 4.6$–14.6 kpc, has DM $= 71$ cm^{-3} pc, while our model yields $DM_{-} = 208$ cm^{-3} pc. This results in a mean electron density of $n_e < 0.016$ cm^{-3} over at least a 4.5 kpc path length! Further timing parallaxes for this pulsar could confirm this unusual result.

While low-DM outliers are difficult to explain, high-DM outliers are likely to arise from the passage of the pulsar line of sight through a dense H II region. Of the 13 high outliers, four are associated with SNRs (Vela, MSH 15−52, G308.8−0.1, and W28) and one has a 10 $M_{\odot}$ companion (and presumably an associated H II region). Using the ionizing output luminosities tabulated by Osterbrock (1989), the dispersion measure of an H II region around an O9 star, for example, would be DM $= 2nR_S = 315$ cm^{-3} pc, where R_S is the Strömgren radius. The excess dispersion measure, defined as $DM_{excess} = DM_{data} - DM_{+}$ for the 13 high outliers, range over $DM_{excess} = 7$–578 cm^{-3} pc. Thus, these lines of sight are consistent with the intersection of the sight line with discrete H II regions. However, we have searched catalogs of diffuse H II regions (Lockman, Pisano, & Howard 1996) and the WHAM maps (Haffner 2000) for correlations with the northern declination pulsars in this sample, and nothing outstanding was found. Since the majority of these pulsars lie at southern declinations, the high angular resolution Hα maps of Gaustad et al. (1997) will be extremely useful in the future.

There are two outliers for which we suspect the distance estimate may be incorrect. The distance to B0656+14 was obtained using an X-ray luminosity model. Given the number of assumptions necessary to estimate the X-ray luminosity of a neutron star, we have some concerns about the reliability of this method. The distance to B0823+26 is based on a parallax measurement by Gwinn et al. (1986). Since the other pulsar examined in that study (B0950+08) has had a significant revision in its distance, a reconsideration of this pulsar parallax may be in order.

We have also compared with the 29 pulsars for which there are only upper or lower limits. We found that 26 of these limits are satisfied by the model, while those for B2020+28 ($D > 3.1$ kpc), B2016+28 ($D > 3.2$ kpc), and B1818−04 ($D < 1.6$ kpc) are not. Thus, our model satisfies the distance constraints for 91 out of 109 pulsars.

4.2. *Spatial Distribution of Residuals*

We now consider whether the known asymmetries in the distribution of Galactic H II regions are reflected in the current data set. A plot of DM_{data}/DM_{model} versus Galactic location is presented in Figure 5, with the spiral arm positions used by TC overlaid. There seem to be two lines of pulsars with a higher than expected dispersion measure, marked by dashed lines. Some of these pulsars have been discussed by Johnston et al. (2001) as particularly noticeable outliers. One of these groups agrees roughly with the posi-

TABLE 3

OUTLIER PULSARS

PSR	l (deg)	b (deg)	D[a] (kpc)	DM_{data} (cm^{-3} pc)	DM_{-}[b] (cm^{-3} pc)	DM_{+}[b] (cm^{-3} pc)	DM_{excess} (cm^{-3} pc)	Method[c]
0656+14......	201.11	8.26	0.18	14.0	3.3	6.2	7.8	X
0833−45......	263.55	−2.79	0.25	68.2	4.9	9.0	59.2	Vela SNR
1741−11......	14.79	9.18	0.36	3.1	6.3	11.7	−3.2	TP
0823+26......	197.00	31.70	0.36	19.5	4.9	9.1	10.4	Π
1259−63......	304.20	−0.99	1.10	146.7	22.8	42.4	104.3	SP
1807−24......	5.80	−2.20	2.50	134.0	44.8	83.2	50.8	NGC 6544
1054−62......	290.30	−3.00	2.70	321.0	40.2	74.6	246.4	K
1900+01......	35.70	−2.00	3.40	246.4	57.5	106.8	139.6	K
1859+07......	40.60	1.10	3.75	261.0	75.1	139.4	121.6	K
1509−58......	320.32	−1.16	4.40	253.2	84.3	156.6	96.6	MSH 15−52 SNR
1641−45......	339.20	−0.20	4.60	475.0	179.2	332.8	142.2	K
1718−35......	351.70	0.70	4.80	496.0	137.9	256.0	240.0	K
1758−23......	6.80	−0.10	5.20	1074.0	266.9	495.6	578.4	K, W28
1338−62......	308.73	−0.04	6.90	730.0	204.5	379.8	350.2	G308.8−0.1 SNR
1937+21......	57.51	−0.29	9.70	71.0	207.6	385.5	−136.6	K, TP

[a] For pulsars with kinematic distances, $D = 0.5(D_{min} + D_{max})$.
[b] $DM_{\pm} = (1 \pm A)DM_{model}(D)$
[c] See Table 1 for list of methods.

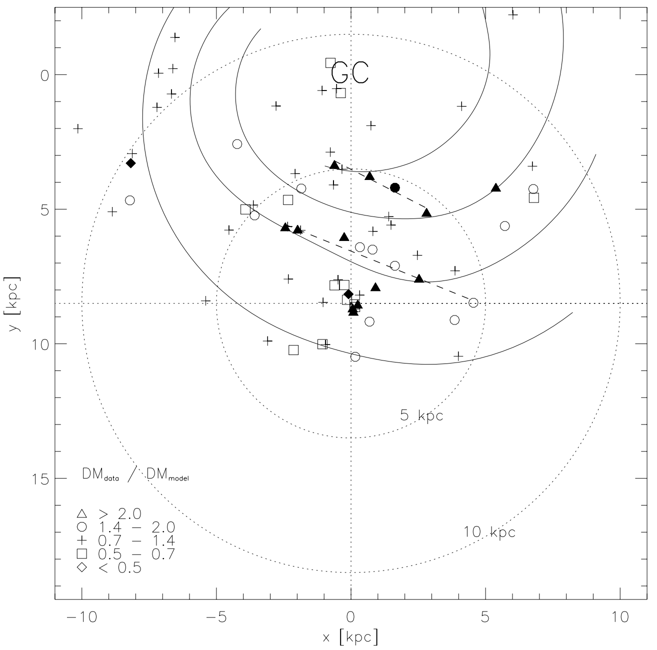

FIG. 5.—Ratio DM_{data}/DM_{model} for pulsars with $|z| < 300$ pc projected on the Galactic plane. The grid circles are labeled with distance from the Sun. The solid lines trace the center of the spiral arms in the TC model. Pulsars that are identified as outliers in Table 3 have filled symbols. There are two regions of high DM_{data}/DM_{model}, at approximately 2 and 5 kpc from the Sun toward the Galactic center. One of these regions (*dashed lines*) coincides with the position of the Sagittarius-Carina arm.

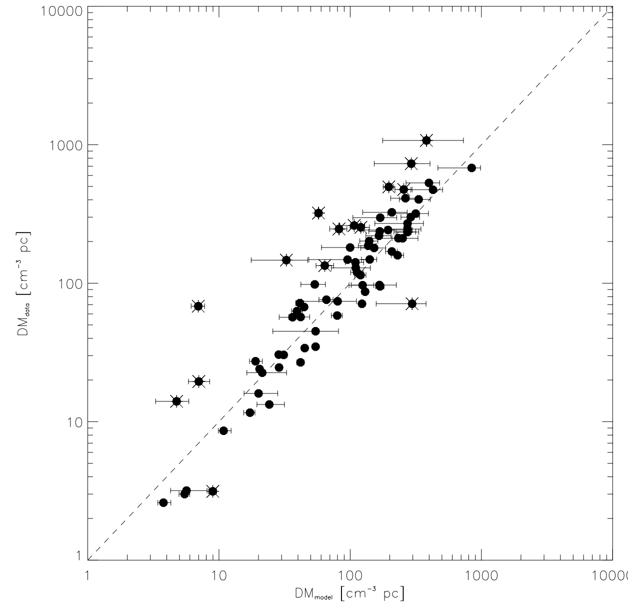

FIG. 6.—DM_{data} vs. DM_{model} for the best-fit model with $f(x) = \mathrm{sech}^2\, x$. The starred points are the pulsars identified as outliers. The error bars shown here only indicate the uncertainties in the distances and do not incorporate our parameterization of scatter in the relationship.

tion of one of the spiral arms and has a pitch angle of 27° from the tangent. The other has a pitch angle of 22° and is not coincident with any of the spiral arms. Given the distance uncertainties for these pulsars, it seems clear that any spiral structure that might exist is only weakly exhibited in this data set.

We have also considered whether there is evidence of a difference in the estimated midplane density if we use only pulsars identified as "interarm pulsars" to estimate the midplane density at the solar neighborhood (Fig. 1, *stars*). We found that there was a slight decrease in the derived midplane density, a factor of $\frac{2}{3}$, compared with the total data set. However, some of these pulsars may lie in or beyond the Local arm, which, although not included in the TC model, is known to exist in the Hα data (Reynolds 1983).

4.3. *Constraints on Clumpiness*

We now consider what factors affect the scatter in the relationship between our simple axisymmetric model and the observed data. Figure 6 shows a comparison between the values of DM_{model} and DM_{data}. DM_{model} takes into account the geometry of the distribution, so it measures the effective integration path. Therefore, we will use it instead of the distance in order to examine the nature of the scatter. An interesting feature in this plot is that the scatter appears to be a fixed fraction of the total dispersion measure.

We considered the possibility that the scatter of DM_{data} about the smooth model might derive from a patchiness in the distribution of electrons in the Galaxy. Such patchiness of the diffuse ionized medium has been predicted, for example, by Miller & Cox (1993), using the observed locations of O stars in the solar neighborhood, and a model for the distribution of the interstellar medium, to calculate the steady state Strömgren volume distribution and ionization.

What would happen if the WIM were *purely* located in discrete lumps (or H II regions)?[3] In this case, we define $\widehat{DM} = DM_{model}$ as the dispersion measure that would result for the average line of sight through some variable number of clumps. The expected total number of lumps intersected along a line of sight would then be $n = \widehat{DM}/DM_{lump}$. The variance in observed number should also be n, so that $(DM_{data} - \widehat{DM})^2 = n DM_{lump}^2 = (\widehat{DM}) DM_{lump}$. We can therefore define a quantity μ for each pulsar,

$$\mu = (DM_{data} - \widehat{DM})^2/\widehat{DM} .$$

If the lump sizes are normally distributed, μ should be independent of $\widehat{DM}$, and its average over a large enough sample of pulsars should be the dispersion measure of the lump. In Figure 7, we plot the running mean of this quantity for both the top-down (from large DM_{model} to small DM_{model}) and bottom-up sums. There is a strong trend in the lump-size estimator with the distance. This could be explained by having two lump populations: small, frequent lumps and large, rarer lumps. Nearby, we pick only small lumps, yielding a small mean. As we move farther away, we pick up more large lumps and the mean value increases. This could explain the steps observed in the bottom-up running mean versus the flatter top-down running mean. We thought that a lognormal distribution with the appropriate shape parameter might have that property but found that a lognormal distribution could almost reproduce the properties of Figure 6 (constant fractional scatter with increasing DM), but not those of Figure 7 (μ is not constant).

[3] Although some authors argue that there is a continuum of power on all scales, here we are considering patches of ionization of finite size.

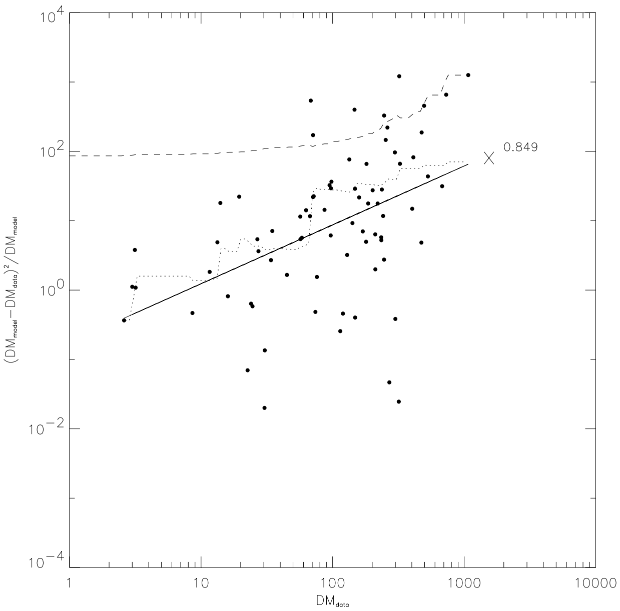

FIG. 7.—Estimation of the mean lump size. The top-down (*dashed line*) and bottom-up (*dotted line*) running averages are shown. If the variance were due to random encounters with lumps along the line of sight, the average of the ordinate should be constant, independent of DM, and roughly equal to the lump size. The solid line is the least-squares fit to the logarithm of the data.

Another possibility is that the deviations of the observed and modeled dispersion measures are not due to statistical noise but, instead, to fractional errors in the distance measurements. In such case, the variance is proportional to $f^2\widehat{\mathrm{DM}}^2$, where f is the approximate fractional error, rather than $\sqrt{n}\mathrm{DM}_{\mathrm{lump}}$. A plot of $(\widehat{\mathrm{DM}} - \mathrm{DM}_{\mathrm{data}})^2/\widehat{\mathrm{DM}}^2$ should then be roughly flat, which is verified in Figure 8. The corresponding value is $f \simeq 30\%$. If distance uncertainties are indeed the main source of scatter, it will be difficult to say

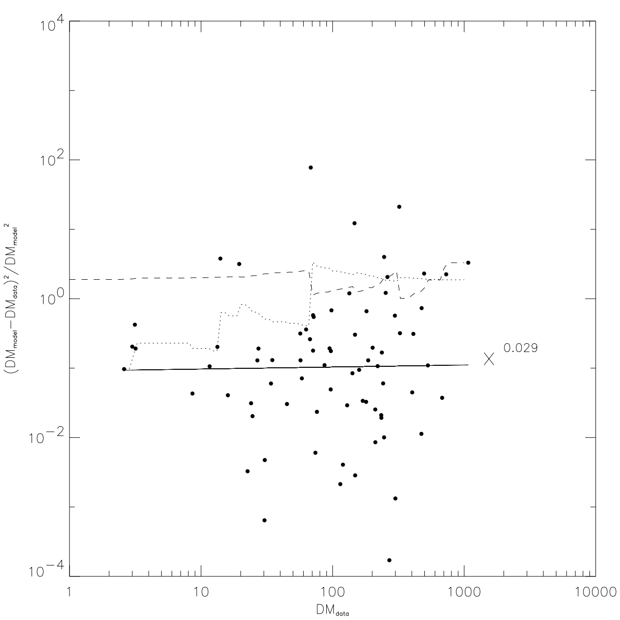

FIG. 8.—Same as Fig. 7, but for the square of the mean fractional error. The slope of the least-squares fit (*solid line*) is close to zero, implying that the dispersion is approximately a constant fraction of DM. We suspect that this behavior is due principally to distance uncertainties.

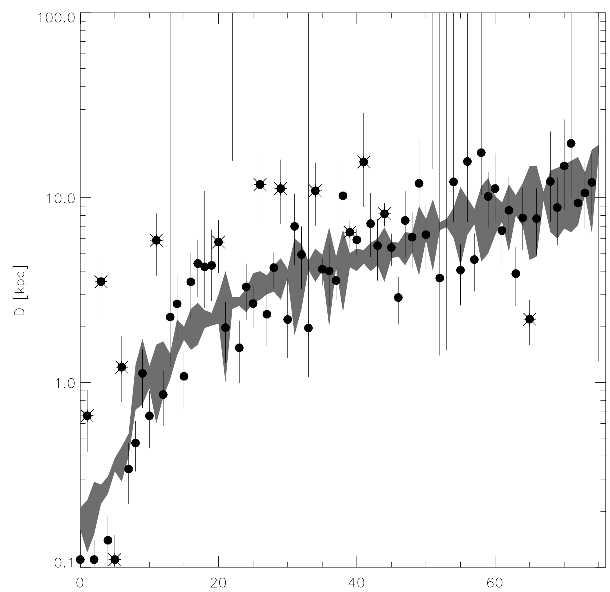

FIG. 9.—Comparison of the predicted and measured distances using the $f(x) = \mathrm{sech}^2\, x$ model. The horizontal axis is the pulsar number, sorted by distance. The gray region is the quoted range in measured distances. The starred points are the outlier pulsars identified in Table 3, and the error bars include the effect of the noise parameter, $A = 0.3$.

anything definitive about the lumpiness of the WIM based on this type of data.

5. PREDICTING PULSAR DISTANCES

One of the principal uses for a model of the Galactic free electron distribution model is to predict the distances to pulsars. While we have not yet introduced the effects of asymmetries, spiral structure, and individual H II regions, we have written two FORTRAN routines (one for each functional form tested) that calculate pulsar distances using

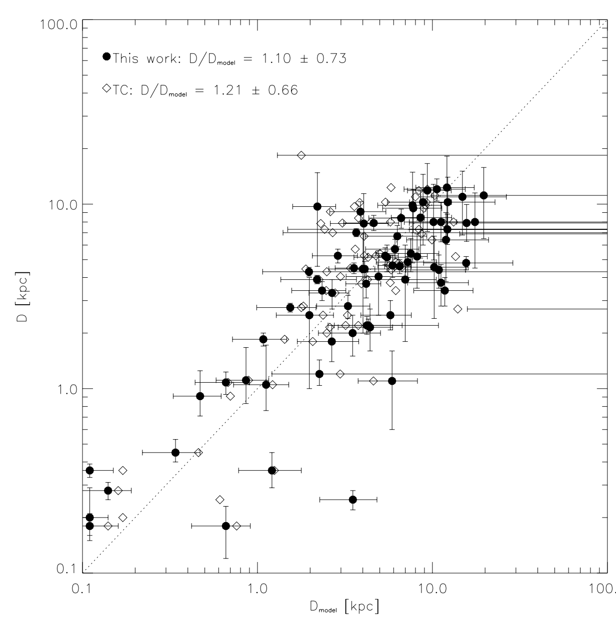

FIG. 10.—Comparison of the predicted and measured distances using both our $f(x) = \mathrm{sech}^2\, x$ model and the Taylor-Cordes model. The horizontal error bars are computed by estimating the distance corresponding to values $\mathrm{DM} = (1 \pm A)\mathrm{DM}_{\mathrm{data}}$. The dispersion in our model is similar to that in the TC model, despite the fact that we have nine fewer adjustable parameters.

the model parameters in Table 2.[4] A comparison of the model distances and true distances for our sample of pulsars is given in Figure 9, using the $f(x) = \mathrm{sech}^2 x$ model. The error bars were obtained by calculating the distance that corresponds to $(1 \pm A)\mathrm{DM}_{\mathrm{data}}$. We note that no pulsars have a dispersion measure higher than the asymptotic limit when the uncertainty associated with our noise parameter A is considered.

In Figure 10, we compare the distances predicted by the TC model and our model with the observed distance constraints. When we consider only those pulsars with allowed DM (smaller than the asymptotic value), the dispersion in our model is similar to that in the model of TC, but with fewer free parameters.

We note however that the model we have developed is relatively unconstrained for pulsars interior to a Galactocentric radius of $R \sim 4$ kpc and exterior to 12 kpc. For example, unlike Taylor & Cordes, we have not included an annulus of electron density at $R = 4$ kpc, which presumably would be associated with the molecular ring. Lazio & Cordes (1998b, 1998d) have discussed how additional information can be used to constrain these regions. We intend to address these issues in the future when we address the nonaxisymmetric structure using the Wisconsin Hα survey.

6. CONCLUSIONS

A smooth model for the distribution of Galactic free electrons was obtained from a set of 109 pulsars with independent distance information. Although a more complex model incorporating spiral arms might be possible, we do not think that it would be well constrained by these pulsar data alone, so we chose to use a simpler and probably more robust functional form. The exponential scale height obtained is consistent with the value quoted by Reynolds (1997). The scatter parameter found ($A = 0.3$) is smaller than that found by Savage et al. (1990). This parameter is used to predict a range of confidence in the predicted distances to pulsars.

Of pulsars with both upper and lower distance limits, 15 are identified as outliers, with 13 of these showing excess dispersion measure. Some of these are associated with supernova remnants or known H II regions. There is one very unusual pulsar, B1937+21, with an extremely low dispersion measure given its distance. In examining the residuals, we identified two regions of enhanced electron density, one of which corresponds well to the expected position of the Sagittarius-Carina spiral arm.

We found that a simple probabilistic model for a lumpy warm ionized medium failed to reproduce the deviations of the observed data from the smooth model. We suspect that the main source of scatter in our model is due to distance uncertainties, although it seems clear that are also occasionally large anomalous dispersion measures associated with H II regions. Some of these are in spiral arms, but their distribution may not be uniform in these arms.

We are grateful to Ron Reynolds, Matt Haffner, Joel Weisberg, and Linda Sparke for useful advice and encouragement, to the NASA Astrophysics Theory Program for financial support under grant NAG 5-8417, and to Mexico's Consejo Nacional de Ciencia y Tecnología for support to G. C. G.

[4] These programs may be obtained by contacting the authors or at the World Wide Web site http://wisp5.physics.wisc.edu/~gomez/publica.html.

REFERENCES

Ables, J. G., & Manchester, R. N. 1976, A&A, 50, 177
Alcaino, G. 1983, A&AS, 52, 105
Alcaino, G., Buonanno, R., Caloi, V., Castellani, V., Corsi, C. E., Iannicola, G., & Liller, W. 1987, AJ, 94, 917
Armandroff, T. E. 1988, AJ, 96, 588
Backer, D. C., & Sramek, R. A. 1982, ApJ, 260, 512
Bailes, M., Manchester, R. N., Kesteven, M. J., Norris, R. P., & Reynolds, J. E. 1990, Nature, 343, 240
Bell, J. F., & Bailes, M. 1996, ApJ, 456, L33
Blair, W. P., Kirshner, R. P., Fesen, R. A., & Gull, T. R. 1984, ApJ, 282, 161
Booth, R. S., & Lyne, A. G. 1976, MNRAS, 174, 53P
Brisken, W. F., Benson, J. M., Beasley, A. J., Fomalont, E. B., Goss, W. M., & Thorsett, S. E. 2000, ApJ, 541, 959
Brocato, E., Buonanno, R., Malakhova, Yu., & Piersimoni, A. M. 1996a, A&A, 311, 778
Brocato, E., Castellani, V., & Ripepi, V. 1996b, AJ, 111, 809
Buonanno, R., Caloi, V., Castellani, V., Corsi, C., Fusi Pecci, F., & Gratton, R. 1986, A&AS, 66, 79
Camilo, F., Foster, R. S., & Wolszczan, A. 1994, ApJ, 437, L39
Campbell, R. M. 1995, Ph.D. thesis, Harvard Univ.
Campbell, R. M., Bartel, N., Shapiro, I. I., Ratner, M. I., Cappallo, R. J., Whitney, A. R., & Putnam, N. 1996, ApJ, 461, L95
Caraveo, P. A. 2000, in IAU Colloq. 177, Pulsar Astronomy: 2000 and Beyond, ed. M. Kramer, N. Wex, & R. Wielebinski (ASP Conf. Ser. 202) (San Francisco: ASP), 289
Caraveo, P. A., Bignami, G. F., Mignani, R., & Taff, L. G. 1996, ApJ, 461, L91
Caswell, J. L., Kesteven, M. J., Komesaroff, M. M., Haynes, R. F., Milne, D. K., Stewart, R. T., & Wilson, S. G. 1987, MNRAS, 225, 329
Caswell, J. L., Kesteven, M. J., Stewart, R. T., Milne, D. K., & Haynes, R. F. 1992, ApJ, 399, L151
Caswell, J. L., Murray, J. D., Roger, R. S., Cole, D. J. & Cooke, D. J. 1975, A&A, 45, 239
Cha, A. N., Sembach, K. R., & Danks, A. C. 1999, ApJ, 515, L25
Chatterjee, S., Cordes, J. M., Lazio, T. J. W., Goss, W. M., Fomalont, E. B., & Benson, J. M. 2001, ApJ, 550, 287
Clifton, T. R., Frail, D. A., Kulkarni, S. R., & Weisberg, J. M. 1988, ApJ, 333, 332
Cordes, J. M., & Rickett, B. J. 1998, ApJ, 507, 846
Cordes, J. M., Weisberg, J. M., Frail, D. A., & Spangler, S. R., & Ryan, M. 1991, Nature, 354, 121
Cox, D. P., & Reynolds, R. J. 1987, ARA&A, 25, 303
Cudworth, K. M., & Rees, R. 1990, AJ, 99, 1491
D'Amico, N., Lyne, A. G., Manchester, R. N., Possenti, A., & Camilo, F. 2001, ApJ, 548, L171
de Jager, G., Lyne, A. G., Pointon, L., & Ponsonby, J. E. B. 1968, Nature, 220, 128
Deshpande, A. A., & Ramachandran, R. 1998, MNRAS, 300, 577
Durrell, P. R., & Harris, W. E. 1993, AJ, 105, 1420
Encrenaz, P. & Guélin, M. 1970, Nature, 227, 476
Feast, M. W., & Walker, A. R. 1987, ARA&A, 25, 345
Fesen, R. A., Winkler, P. F., Rathore, Y., Downes, R. A., Wallace, D., & Tweedy, R. W. 1997, AJ, 113, 767
Fich, M., Blitz, L., & Stark, A. A. 1989, ApJ, 342, 272
Finley, J. P. & Ögelman, H. 1994, ApJ, 434, L25
Frail, D. A., Cordes, J. M., Hankins, T. H., & Weisberg, J. M. 1991, ApJ, 382, 168
Frail, D. A., Goss, W. M., & Whiteoak, J. B. Z. 1994, ApJ, 437, 781
Frail, D. A., Kulkarni, S. R., & Vasisht, G. 1993, Nature, 365, 136
Frail, D. A., & Weisberg, J. M. 1990, AJ, 100, 743 (FW90)
Fomalont, E. B., Goss, W. M., Beasley, A. J., & Chatterjee, S. 1999, AJ, 117, 3025
Gaensler, B. M., & Johnston, S. 1995, MNRAS, 275, L73
Gaustad, J., Rosing, W., Chen, G., McCullough, P. & van Buren, D. 1997, BAAS, 190, No. 30.05
Georgelin, Y. M., & Georgelin, Y. P. 1976, A&A, 49, 57
Georgelin, Y. M., Russeil, D., Amram, P., Georgelin, Y. P., Marcelin, M., Parker, Q. A., & Viale, A. 2000, A&A, 357, 308
Gómez-González, J., Falgarone, E., Encrenaz, P., & Guélin, M. 1972, Astrophys. Lett., 12, 207
Gómez-González, J., & Guélin, M. 1974, A&A, 32, 441
Gómez-González, J., Guélin, M., Falgarone, E., & Encrenaz, P. 1973, Astrophys. Lett., 13, 229
Golden, A., & Shearer, A. 1999, A&A, 342, L5
Gordon, C. P., Gordon, K. J., & Shalloway, A. M. 1969, Nature, 222, 129
Gordon, K. J., & Gordon, C. P. 1970, Astrophys. Lett., 5, 153

Gordon, K. J., & Gordon, C. P. 1973, A&A, 27, 119
———. 1975, A&A, 40, 27
Graham, D. A., Mebold, U., Hesse, K. H., Hills, D. L., & Wielebinski, R. 1974, A&A, 37, 405
Guélin, M., Encrenaz, P., & Bonazzola, S. 1971, A&A, 14, 387
Guélin, M., Guibert, J., Huchtmeier, W., & Weliachew, L. 1969, Nature, 221, 249
Gupta, Y. 1995, ApJ, 451, 717
Gwinn, C. R., Taylor, J. H., Weisberg, J. M., & Rawley, L. A. 1986, AJ, 91, 338 (erratum 91, 974)
Haffner, L. M. 2000, in ASP Conf. Ser. 231, Tetons 4: Galactic Structure, Stars, and the Interstellar Medium, ed. C. E. Woodward, M. D. Bicay, & J. M. Shull (San Francisco: ASP), in press
Harris, W. E. 1996, AJ, 112, 1487
Heiles, C., Kulkarni, S. R., Stevens, M. A., Backer, D. C., Davis, M. M., & Goss, W. M. 1983, ApJ, 273, L75
Heitsch, F., & Richtler, T. 1999, A&A, 347, 455
Hesser, J. E., Harris, W. E., VandenBerg, D. A., Allwright, J. W. B., Shott, P., & Stetson, P. B. 1987, PASP, 99, 739
Johnston, S., Koribalski, B., Weisberg, J. M., & Wilson, W. 1996, MNRAS, 279, 661
———. 2001, MNRAS, 322, 715
Johnston, S., Manchester, R. N., Lyne, A. G., Nicastro, L., & Spyromilio, J. 1994, MNRAS, 268, 430
Kaspi, V. M., Crawford, F., Manchester R. N., Lyne, A. G., Camilo, F., D'Amico, N., & Gaensler, B. M. 1998, ApJ, 503, L161
Kaspi, V. M., Manchester, R. N., Johnston, S., Lyne, A. G., & D'Amico, N. 1996, AJ, 111, 2028
Kaspi, V. M., Taylor, J. H., & Ryba, M. F. 1994, ApJ, 428, 713
Koribalski, B., Johnson, S., Weisberg, J. M., & Wilson, W. 1995, ApJ, 441, 756
Kulkarni, S. R., Djorgovski, S., & Klemola, A. R. 1991, ApJ, 367, 221
Lazio, T. J. W., Anantharamaiah, K. R., Goss, W. M., Kassim, N. E., & Cordes, J. M. 1999, ApJ, 515, 196
Lazio, T. J. W., & Cordes, J. M. 1998a, ApJS, 115, 225
———. 1998b, ApJ, 497, 238
———. 1998c, ApJS, 118, 201
———. 1998d, ApJ, 505, 715
Legge, D. 2000, in IAU Colloq. 177, Pulsar Astronomy: 2000 and Beyond, ed. M. Kramer, N. Wex, & R. Wielebinski (ASP Conf. Ser. 202) (San Francisco: ASP), 141
Lockman, F. J., Pisano, D. J., & Howard, G. J. 1996, ApJ, 472, 173
Lorimer, D. R., Lyne, A. G., & Camilo, F. 1998, A&A, 331, 1002
Manchester, R. N., Murray, J. D., & Radhakrishnan, V. 1969, Astrophys. Lett., 4, 229
Manchester, R. N., Wellington, K. J., & McCulloch, P. M. 1981, in IAU Symp. 95, Pulsars: 13 Years of Research on Neutron Stars, ed. W. Sieber & R. Wielebinski (Dordrecht: Reidel), 445
Miller, W. W., III, & Cox, D. P. 1993, ApJ, 417, 579
Ortolani, S., Barbuy, B., & Bica, E. 1994, A&AS, 108, 653
———. 1996, A&A, 308, 733
Osterbrock, D. E. 1989, Astrophysics of Gaseous Nebulae and Active Galactic Nuclei (Mill Valley, CA: Univ. Sci.)
Paltrinieri, B., Ferraro, F. R., Fusi Pecci, F., & Carretta, E. 1998, MNRAS, 293, 434
Rees, R. F., & Cudworth, K. M. 1991, AJ, 102, 152
Rey, S.-C., Lee, Y.-W., Byun, Y.-I., & Chun, M.-S. 1998, AJ, 116, 1775
Reynolds, R. J. 1983, ApJ, 268, 698
———. 1989, ApJ, 339, L29
———. 1997, in The Physics of Galactic Halos, ed. H. Lesch, R.-J. Dettmar, U. Mebold, & R. Schlickeiser (Berlin: Akad.), 57
Reynolds, R. J., Tufte, S. L., Haffner, L. M., Jaehnig, K., & Percival, J. W. 1998, Publ. Astron. Soc. Australia, 15, 14
Russeil, D., Georgelin, Y. M., Amram, P., Gach, J.-L., Georgelin, Y. P., & Marcelin, M. 1998, A&AS, 130, 119
Ryba, M. F., & Taylor, J. H. 1991, ApJ, 371, 739
Salter, M. J., Lyne, A. G., & Anderson, B. 1979, Nature, 280, 477
Sandhu, J. S., Bailes, M., Manchester, R. N., Navarro, J., Kulkarni, S. R., & Anderson, S. B. 1997, ApJ, 478, L95
Sandquist, E. L., Bolte, M., Stetson, P. B., & Hesser, J. E. 1996, ApJ, 470, 910
Sarajedini, A., & Norris, J. E. 1994, ApJS, 93, 161
Saravanan, T. P., Deshpande, A. A., Wilson, W., Davies, E., McCulloch, P. M., & McConnell, D. 1996, MNRAS, 280, 1027
Savage, B. D., Edgar, R. J., & Diplas, A. 1990, ApJ, 361, 107
Stairs, I. H., Nice, D. J., Thorsett, S. E., & Taylor, J. H. 2000, in Gravitational Waves & Experimental Gravity, ed. J. Trân Thanh Vân, J. Dumarchez, S. Raynoud, C. Salomon, S. Thorsett, & J.-Y. Vinet (Hanoi: Thê Giói), 309
Tauris, T. M., et al. 1994, ApJ, 428, L53
Taylor, J. H., & Cordes, J. M. 1993, ApJ, 411, 674 (TC)
Toscano, M., Britton, M. C., Manchester, R. N., Bailes, M., Sandhu, J. S., Kulkarni, S. R., & Anderson, S. B. 1999, ApJ, 523, L171
Trimble, V., & Woltjer, L. 1971, ApJ, 163, L97
Weisberg, J. M., Boriakoff, V., & Rankin, J. 1979, A&A, 77, 204
Weisberg, J. M., Rankin, J., & Boriakoff, V. 1980, A&A, 88, 84
Weisberg, J. M., Rankin, J. M., & Boriakoff, V. 1987, A&A, 186, 307
Weisberg, J. M., Siegel, M. H., Frail, D. A., & Johnston, S. 1995, ApJ, 447, 204